

QCD Thermodynamics on the Lattice: Recent Results

Carleton DeTar

*Department of Physics and Astronomy, University of Utah, Salt Lake City, Utah 84112, USA **

I give a brief introduction to the goals, challenges, and technical difficulties of lattice QCD thermodynamics and present some recent results from the HotQCD collaboration for the crossover temperature, equation of state, and other observables.

I. INTRODUCTION

Numerical simulations and models have established that the high-temperature behavior of QCD at low baryon number density is governed by two interrelated phenomena, namely the transition from a low temperature, confined regime to a high temperature deconfined regime and the transition from a low temperature regime with spontaneously broken chiral symmetry to a high temperature regime in which the chiral symmetry is restored. The deconfinement phenomenon is especially apparent at very large quark masses where the first order phase transition of pure SU(3) Yang-Mills theory becomes manifest. The chiral restoration phenomenon, on the other hand, is most relevant in the limit of vanishing quark masses. Between these extremes only a nonperturbative calculation can say what happens. The present consensus in lattice QCD is that there is no phase transition — only a crossover — at physical quark masses and zero baryon number density [1, 2].

Figure 1 (left) summarizes in qualitative terms our knowledge of the QCD phase diagram as a function of the light (up, down, and strange) quark masses $m_u = m_d$ and m_s . Lattice calculations aim to check this picture. One important question is whether, when we fix the strange quark mass at

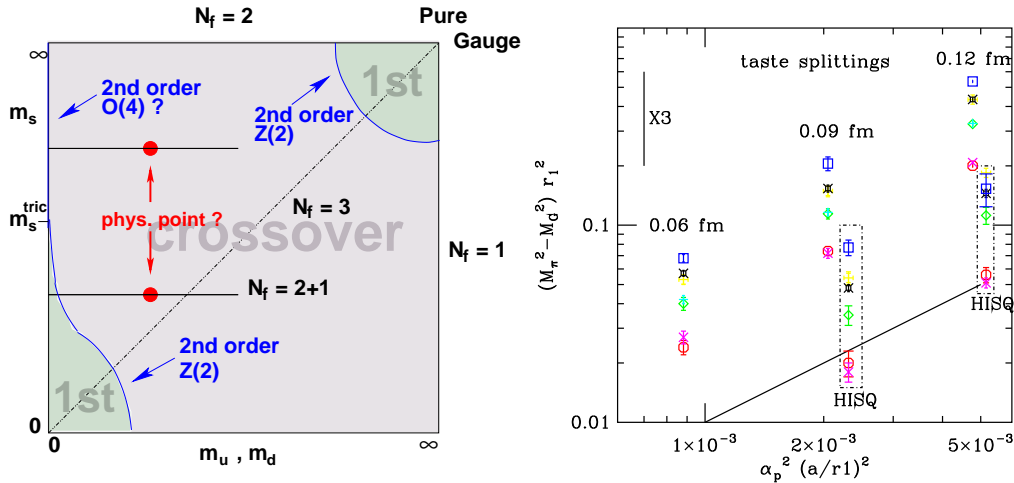


FIG. 1: Left: Sketch of phase diagram at zero baryon density as a function of light quark masses $m_u = m_d$ and m_s . Right: Splitting of the pion taste multiplet showing the expected decrease with lattice spacing. The unboxed points are for the asqtad action and the much lower boxed points are for the HISQ action.

* Temporary address: Center for Computational Sciences, Tsukuba University, Tsukuba, Japan

its physical value and reduce the up and down quark masses, we encounter the first-order transition region. Present indications are that we do not.

What can we learn about QCD thermodynamics from numerical lattice simulations? Here is a list of objectives. More could be added.

- Obtaining accurate values of the crossover temperature T_p .
- Determining the equation of state, velocity of sound, etc.
- Studying critical universality at low light quark masses.
- Calculating transport properties of the plasma.
- Establishing the extent of validity of the hadron resonance gas model at low T .
- Determining the behavior of in-medium hadronic modes (e.g. J/ψ), especially above T_p ?
- Searching for an experimentally accessible critical point at nonzero baryon number density.

For all of these topics a nonperturbative treatment is necessary. Numerical simulation on the lattice gives a first-principles, nonperturbative treatment. We know of no alternative. It does not answer all of our questions, however. Here is a list of limitations:

- We can treat only static thermodynamic equilibrium or small perturbations around it.
- We work in euclidean time: Real time properties are difficult to extract. Transport properties can be computed, in principle, but it is not easy.
- Calculations at nonzero quark number density are very difficult.

Phenomenological models can help extrapolate from lattice results to regimes that are inaccessible to lattice calculations.

II. LATTICE METHODOLOGY

For an introduction to lattice methods for QCD thermodynamics, please see [3] and references therein. Here we mention only a few key concepts.

A. Feynman path integral

We work with quantum grand-canonical partition function

$$Z = \text{Tr} \left[\exp \left(-H/T + \sum_i \mu_i N_i/T \right) \right], \quad (1)$$

for temperature T , QCD hamiltonian H , chemical potential μ_i , and conserved charge N_i . It is rewritten, using the Feynman path integral approach, as the functional integral

$$Z = \int dA_\mu d\psi d\bar{\psi} \exp[-S(A, \psi, \bar{\psi}, \mu)] \quad (2)$$

where A_μ , ψ , $\bar{\psi}$ represent the gluon and quark fields and S is the classical action in a Euclidean space-time (imaginary time). The continuous space-time is discretized as a lattice of points of spacing a , and the classical action is formulated on that lattice. The parameters of the action are, as usual, the gauge coupling and the quark masses. Introducing the lattice puts the functional integration in a form that is more amenable to numerical simulation, and it provides the ultraviolet regulation needed to define QCD.

B. Varying the temperature

The imaginary time coordinate has a finite extent determined by the temperature. So if there are N_τ points in the time direction, at lattice spacing a , the temperature is given by $T = 1/(aN_\tau)$. There are two methods in current use for varying the temperature.

1. Fixed N_τ method. Through the renormalization group, the lattice spacing a depends on the bare gauge coupling g , so as g decreases, a decreases, and T increases. Low T then implies larger lattice spacing and larger cutoff effects! With this method we scan a temperature range at one fixed N_τ and then repeat at larger N_τ to move closer to the continuum.
2. Fixed scale method. [4, 5] With this method we fix the gauge coupling and lattice spacing and vary N_τ . Cutoff effects are then uniform in T .

C. Setting the bare quark masses

Quark masses can also be varied to explore the phase diagram. It is useful to work along “lines of constant physics”; *i.e.* we tune the bare quark masses so as to keep (zero-temperature) meson masses fixed in physical units as T (so a) is varied. Typically we set the strange quark mass m_s to its physical value, but it is expensive to calculate with a physical up and down quark mass $m_u \approx m_d = m_\ell$, so we fix the ratio m_ℓ/m_s , repeat the calculation for a range of ratios, and then extrapolate to the physical point.

D. Determining the lattice scale

To get T in MeV we need to know a in physical units. This value is determined in a zero temperature calculation at the same hamiltonian parameters. It requires matching one dimensionful lattice result with one experimental result. Two common methods are in use:

1. f_K scale. One measures the meson decay constant in lattice units af_K at zero temperature. From the experimental value of f_K , we then know a .

2. r_1 or r_0 method. This method is based on a measurement of the static quark-antiquark potential, a relatively easy process. The constant r_1 is defined as the value of R where $R^2 dV(R)/dR = 1$. The Sommer scale r_0 is similarly defined [6]. Of course, these values are not measured in experiment. So their values are determined in terms of an experimentally observable quantity, such as the splitting of the Υ spectrum, with the result $r_1 \approx 0.31$ fm and $r_0 \approx 0.47$ fm [7].

All scale definitions must agree at zero lattice spacing and physical quark masses, but we expect some disagreement at nonzero spacing and unphysical masses. With current methods we can get better than $\sim 2\%$ accuracy in T .

E. Lattice fermion doubling problem

Putting fermions on the lattice is nontrivial. Discretization of the Dirac action introduces complications. As a result there are several lattice fermion formulations, each with its advantages and disadvantages. With a naive discretization in three space and one time dimension we get 2^4 quark species of the same mass. This is called the fermion “doubling” problem. The remedial strategy varies with the fermion implementation.

Wilson introduced a dimension-five term in the action to lift the degeneracy. All unwanted fermions then get masses of order $1/a$. This procedure breaks chiral symmetry explicitly, which adds to the complexity of studies at finite temperature.

The domain wall and overlap implementations usually start from Wilson’s action and build from it an action with a form of chiral symmetry. It is rigorous, elegant, but computationally expensive.

The staggered fermion implementation diagonalizes the fermion matrix partially to reduce the degeneracy from 16 to 4. In modern language, these are called “tastes”. (Then each flavor comes in four tastes.) Finally, one takes the fourth root of the fermion determinant to get an approximately correct counting of sea quark flavors. This is a controversial step, but recent work has placed it on firmer theoretical ground. (See a discussion and references in [7].)

The lattice regulates ultraviolet divergences by introducing a momentum cutoff of order $1/a$. As the spacing is reduced, we remove the cutoff. Depending on how the lattice action is formulated, at nonzero lattice spacing, results can be distorted by the cutoff. The goal of improving the formulation is to reduce these effects at a given a . This is done by adding irrelevant higher-dimensional terms to the action [8]. The original staggered fermion action is “unimproved”: good to $\mathcal{O}(a^2)$. Improved formulations in current wide use are called “p4” [9, 10], “asqtad” (for references, see [7]), “stout” [11, 12], and “HISQ” [13].

In the continuum limit the tastes are described by an exact, extraneous $SU(4)$ symmetry, and the fourth root is trivial. At nonzero lattice spacing, this symmetry is broken, which leads to a distortion of the hadron spectrum, as shown below. As we will see, recent calculational results suggest that taste symmetry breaking is the source of a large share of the cutoff effects in traditional staggered fermion thermodynamics. Currently, the HISQ action has the most improved taste symmetry, followed closely behind by stout, and then asqtad, and p4. Aside from taste splitting,

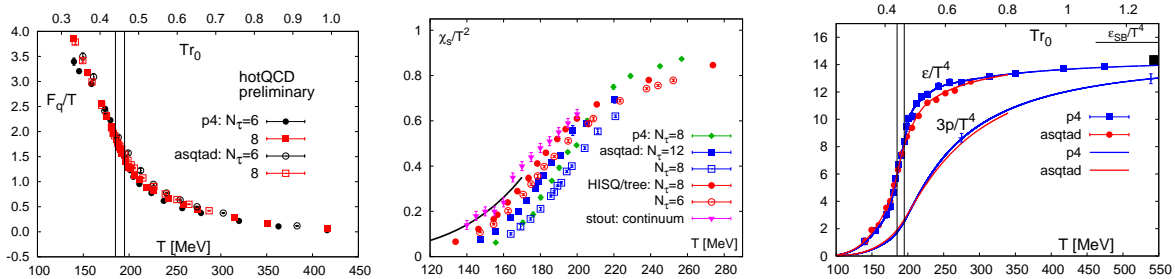


FIG. 2: Three deconfinement markers as a function of temperature (MeV). Left: static quark free energy [3]. Middle: strange quark number susceptibility [14]. Right: energy density and pressure in units of temperature [22]. The Stefan-Boltzmann free-gas limit is indicated on the right. The crossover is evident in all of them.

other cutoff effects are expected. The p4, asqtad, and HISQ actions are all improved with leading errors at $\mathcal{O}(a^2\alpha_s)$, and the stout action is less improved with leading errors at $\mathcal{O}(a^2)$.

The effects of taste-symmetry breaking are most evident in the pion spectrum. Four tastes of quarks and four of antiquarks yield a multiplet of sixteen pion tastes for each physical pion. The resulting multiplet structure is shown in Fig. 1 [14]. The figure shows that the splitting decreases approximately as $a^2\alpha_s^2$. The considerable improvement of HISQ over asqtad is also apparent.

III. RESULTS

I will review some recent results mostly from the HotQCD collaboration [24] including some very new ones based on the HISQ action $N_\tau = 6, 8$ and asqtad $N_\tau = 12$.

A. Indicators of deconfinement

A variety of observables are good phenomenological indicators of deconfinement. We discuss two of them, namely the Polyakov loop or “static quark self energy” and the strange quark number susceptibility. A third, the equation of state, is discussed later below.

The traditional deconfinement indicator is the “Polyakov loop” L . It is related to the static quark free energy F_q , *i.e.* the difference of the free energy of the thermal ensemble with and without a static quark:

$$L = \left\langle \text{Tr} P \exp\left(ig \int_0^{1/T} d\tau A_0(\tau)\right) \right\rangle \sim \exp[-F_q(T)/T] \quad (3)$$

Even when light quarks are present in the ensemble, adding a static quark at low temperature requires screening by a light quark, increasing the free energy by an amount equal, roughly, to a constituent quark mass. In the deconfined phase the constituent quark mass is very low. This effect is visible in the left panel of Fig. 2. There is no direct linkage between this quantity and the chiral order parameter, so this observable is not a good indicator of the chiral transition.

The strange quark number susceptibility measures fluctuations in strangeness $\chi_s = \langle S^2 \rangle / (VT)$. Such fluctuations are expected to be large in the deconfined phase where strangeness is carried by

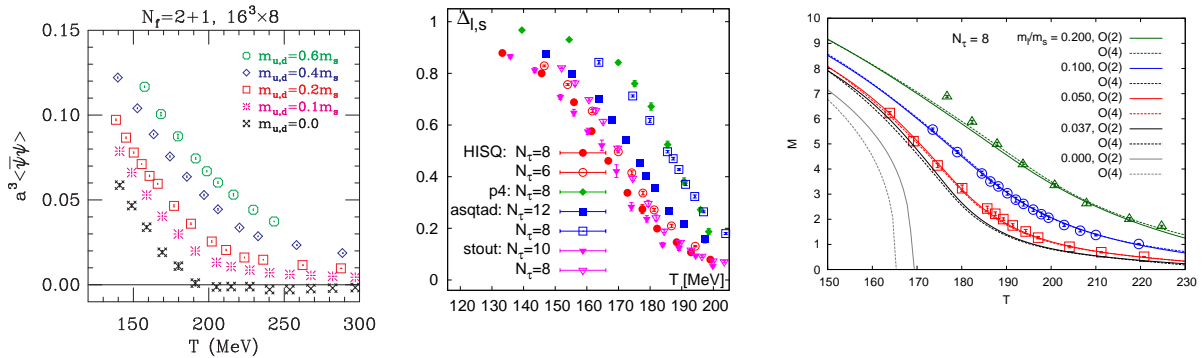


FIG. 3: Left: Chiral condensate for a variety of quark mass ratios m_ℓ/m_s [20]. Also shown is the extrapolation to zero quark mass where a singularity is expected to appear. Middle: The subtracted chiral condensate (see text) from various fermion formulations, showing a lowering of the transition temperature with decreased taste splitting [17]. Right: Chiral condensate for the asqtad action fit to the O(2) and O(4) critical scaling functions (see text) [17].

the quark degrees of freedom, and small in the confined phase where it is carried by hadrons containing a strange quark. This behavior is apparent in the right panel of Fig. 2. Although this quantity is expected to have a singularity at the chiral critical point, an analysis of critical behavior suggests that the singularity is too mild to make this observable a good indicator of the chiral transition.

B. Indicators of chiral symmetry restoration

The chiral condensate and its associated susceptibility are obvious markers of chiral symmetry restoration. The light quark chiral condensate $\bar{\psi}\psi$ is, in fact, the order parameter for chiral symmetry at zero up and down quark masses.

$$\langle \bar{\psi}\psi \rangle = (T/V) \partial \log Z / \partial m. \quad (4)$$

It is nonzero when chiral symmetry is spontaneously broken and zero when it is restored. We expect restoration at high T . When all sea quark masses are nonzero, chiral symmetry is not exact, so we don't get zero, exactly. The example in Fig. 3 (left) confirms the expected behavior.

The chiral condensate is subject to both additive (divergent at nonzero quark mass) and multiplicative renormalization. To compare results for different actions, it is necessary to remove these factors. A convenient choice is the “subtracted” condensate (middle panel of Fig. 3):

$$\Delta_{\ell,s} = [(\langle \bar{\psi}\psi \rangle)_\ell(T) - m_\ell/m_s (\langle \bar{\psi}\psi \rangle)_s(T)] / [(\langle \bar{\psi}\psi \rangle)_\ell(T=0) - m_\ell/m_s (\langle \bar{\psi}\psi \rangle)_s(T=0)] \quad (5)$$

C. Taste symmetry and the transition temperature

In Fig. 2 and Fig. 3 we see that the various actions give strikingly different. The discrepancies correlate with the degree of taste symmetry of the action. As taste symmetry is improved, the

curves shift to lower temperature. This is achieved by decreasing the lattice spacing, *i.e.*, increasing N_τ and by improving the action. For the latter property, in order of gradually improved taste symmetry, the actions are p4, asqtad, stout, and HISQ.

D. Scaling of chiral order parameter (Magnetic equation of state)

At zero quark mass we expect universal $O(4)$ critical behavior at the chiral-symmetry-restoring phase transition. It is $O(2)$ at nonzero lattice spacing for staggered fermion actions. Define

$$t = (T - T_c)/T_c \quad \text{and} \quad h = (m_\pi/m_K)^2 \approx m_\ell/m_s \quad (6)$$

For small h and t we have

$$M(t, h) \equiv m_s/T^4 \langle \bar{\psi}\psi(t, h) \rangle \rightarrow t^\beta f(z) + \text{regular} \quad (7)$$

where $z = z_0 t/h^{1/(\beta\delta)}$ and $f(z)$ is the universal scaling function for $O(2)$ or $O(4)$. This analysis is tested in Fig. 3 (right). It follows the analysis for the p4 action described in [16]. A similar analysis for Wilson fermions long ago found surprisingly good scaling [15]. Such a scaling analysis gives a framework for extrapolating results to the physical quark mass.

E. Chiral susceptibility

The chiral susceptibility measures fluctuations in the chiral condensate. For light quarks it is

$$\chi_\ell = \frac{T}{V} \frac{\partial^2}{\partial m_\ell^2} \log Z = \chi_{\ell, \text{disc}} + 2\chi_{\ell, \text{conn}}. \quad (8)$$

The “disconnected” and “connected” labels refer to the topology of quark world lines in the conventional computation. The disconnected term peaks at the crossover, as shown in Fig. 4. The peak height diverges in the chiral limit. Thus it is an excellent marker for the crossover. Consistent with the behavior of chiral condensate, the peak shifts to lower temperature as the lattice spacing is decreased (increasing N_τ).

F. Transition temperature at the physical point

Locating the peaks of the chiral susceptibility at other quark masses and lattice spacings allows us to carry out an extrapolation to the physical light quark mass (approximately $m_s/27$) and zero lattice spacing. The temperature at the peak is plotted in Fig. 4 (right) together with curves based on the ansatz

$$T_p = T_c(0) + a(m_\ell/m_s)^{1/(\beta\delta)} + b/N_\tau^2 \quad (9)$$

The light quark mass dependence is motivated by the expected universal $O(4)$ critical behavior ($1/(\beta\delta) = 0.54$) and the lattice spacing ($1/N_\tau$) dependence is based on the expected $O(a^2)$ cutoff dependence of the action.

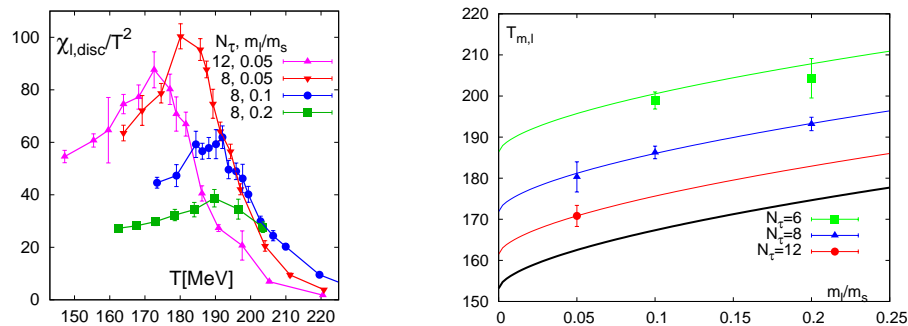


FIG. 4: Left: Disconnected light quark chiral susceptibility for the asqtad action showing a peak at the crossover temperature [18]. The peak shifts to lower temperatures with increasing N_τ (decreasing lattice spacing). Right: The crossover temperature as a function of the light quark mass ratio and N_τ [18]. The curves show the fit to Eq. (9).

At the physical point $m_\ell/m_s = 1/27$ and zero lattice spacing we obtain a preliminary value of the crossover temperature at the physical point: $T_p(\text{phys}) \approx 164(6)$ MeV [18]. The Budapest-Wuppertal result for a closely related observable is $147(2)(3)$ MeV [19]

In the past couple of years there has been a lively discussion about the transition temperature. In 2004 the MILC collaboration, using the improved asqtad action, carried out a similar extrapolation from $N_\tau = 4, 6$, and 8 to the physical point with lower statistics than in the present study and reported $169(12)(4)$ MeV [20]. In 2006 Cheng *et al.*, using the p4 action, reported $192(7)(4)$ MeV at the physical point based on simulations at $N_\tau = 4$ and 6 [21]. The HotQCD collaboration published a study of the equation of state in 2009, based on both the asqtad and p4 actions, but, because there were not enough data to do so at the time, quite deliberately did not quote a result for the transition temperature at the physical point [22]. At the same time the Budapest-Wuppertal collaboration reported on its study using the stout action, with several values depending on the observable, including $147(2)(3)$ MeV from their renormalized disconnected susceptibility and $165(5)(3)$ from the strange quark number susceptibility [19].

What we have learned first from these studies is that the transition temperature is more sensitive to taste-breaking effects in the staggered action than some had expected. But the story is not finished. The HotQCD collaboration has undertaken a more comprehensive analysis of $O(N)$ universality with its current data. This study may lead to a more refined determination of the crossover temperature. It also provides a means of deciding which observables are better markers of critical behavior.

G. Equation of state (trace anomaly)

The equation of state, *i.e.*, the energy density ϵ , pressure p , and entropy density s as a function of temperature is an important quantity in the hydrodynamics of heavy ion collisions and in the characterization of the early universe. The now standard lattice QCD construction of the equation of state begins with a calculation of the “trace anomaly” or “interaction measure”, $I = \epsilon - 3p$. It

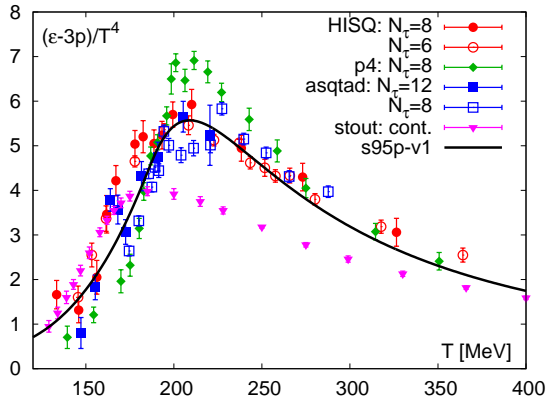


FIG. 5: Interaction measure in units of temperature *vs.* temperature for the asqtad, p4, HISQ, and stout actions at a variety of values of N_τ [17]. The curve is a convenient parameterization. It agrees with the hadron resonance gas model at low temperature.

is plotted in Fig. 5 for a variety of actions. At low temperature the measured points lie below the prediction of the hadron resonance gas model (based on physical hadron masses). Such an effect is an expected consequence of the splitting of the pion taste multiplet, which tends to increase the rms mass of the pion, and therefore increase the transition temperature. At high temperature where cutoff effects are much reduced, the three actions (p4, asqtad, and HISQ) agree. However, a recent Budapest-Wuppertal result for the stout action shows a significant deviation [23]. The results are compared in Fig. 5. The stout action points include a rather large “tree-level” correction for cutoff effects. Since the p4, asqtad, and HISQ actions are improved at $\mathcal{O}(a^2)$, they have better scaling properties at high temperature, as shown, and no such correction was applied. In any case the correction vanishes for all actions in the continuum limit.

The pressure p and energy density ϵ are obtained from the interaction measure I as follows:

$$p = \frac{T}{V} \int_{T_0}^T dT' \frac{1}{T'^3} I(T') \quad \epsilon = I + 3p \quad (10)$$

Results are shown on the right in Fig. 2 for the asqtad and p4 actions.

IV. CONCLUSIONS

Lattice QCD is providing a wealth of information about high temperature QCD, particularly about the nature of the transition from low to high temperature and the behavior of several quantities of phenomenological importance, including the equation of state and the quark number susceptibility. Other quantities I did not have space to discuss are the speed of sound, the equation of state at nonzero baryon density, transport properties, and the survival of hadronic modes in the medium.

The staggered fermion formulation is most widely used for thermodynamic studies. We have learned that taste-symmetry breaking makes a large contribution to cutoff effects in that formulation making it highly desirable to use actions such as HISQ and stout that have better taste

symmetry.

More is yet to be learned about the critical scaling of various quantities near the chiral phase transition, and further study is needed to settle substantial disagreements in the interaction measure at moderate temperature.

-
- [1] R. Hwa and X.N. Wang, ed., *Quark Gluon Plasma 4*, (World Scientific, Singapore, 2010).
 - [2] K. Yagi, T. Hatsuda, and Y. Miake, “Quark Gluon Plasma: From big bang to little bang” (Cambridge University Press, Cambridge, 2008).
 - [3] C. DeTar and U. M. Heller, *Eur. Phys. J. A* **41**, 405 (2009) [arXiv:0905.2949 [hep-lat]].
 - [4] L. Levkova, *Nucl. Phys. Proc. Suppl.* **119**, 520 (2003) [arXiv:hep-lat/0209069].
 - [5] T. Umeda, S. Ejiri, S. Aoki, T. Hatsuda, K. Kanaya, Y. Maezawa and H. Ohno, *Phys. Rev. D* **79**, 051501 (2009) [arXiv:0809.2842 [hep-lat]].
 - [6] R. Sommer, *Nucl. Phys. B* **411**, 839 (1994) [arXiv:hep-lat/9310022].
 - [7] A. Bazavov *et al.*, *Rev. Mod. Phys.* **82**, 1349 (2010) [arXiv:0903.3598 [hep-lat]].
 - [8] K. Symanzik, *Nucl. Phys. B* **226**, 205 (1983).
 - [9] U. M. Heller, F. Karsch and B. Sturmfels, *Phys. Rev. D* **60**, 114502 (1999) [arXiv:hep-lat/9901010].
 - [10] F. Karsch, E. Laermann and A. Peikert, *Phys. Lett. B* **478**, 447 (2000) [arXiv:hep-lat/0002003].
 - [11] C. Morningstar and M. J. Peardon, *Phys. Rev. D* **69** (2004) 054501 [arXiv:hep-lat/0311018].
 - [12] Y. Aoki, Z. Fodor, S. D. Katz and K. K. Szabo, *JHEP* **0601**, 089 (2006) [arXiv:hep-lat/0510084].
 - [13] E. Follana *et al.* [HPQCD Collaboration and UKQCD Collaboration], *Phys. Rev. D* **75**, 054502 (2007) [arXiv:hep-lat/0610092].
 - [14] A. Bazavov *et al.* [MILC collaboration], *Phys. Rev. D* **82**, 074501 (2010) [arXiv:1004.0342 [hep-lat]].
 - [15] Y. Iwasaki, K. Kanaya, S. Kaya and T. Yoshie, *Phys. Rev. Lett.* **78**, 179 (1997) [arXiv:hep-lat/9609022].
 - [16] S. Ejiri *et al.*, *Phys. Rev. D* **80**, 094505 (2009) [arXiv:0909.5122 [hep-lat]].
 - [17] A. Bazavov and P. Petreczky [HotQCD collaboration], (PoS LAT2010, to be published, 2010).
 - [18] W. Söldner [HotQCD collaboration], (PoS LAT2010, to be published, 2010).
 - [19] S. Borsanyi, Z. Fodor, C. Hoelbling, S. D. Katz, S. Krieg, C. Ratti and K. K. Szabo [Wuppertal-Budapest Collaboration], *JHEP* **1009**, 073 (2010) [arXiv:1005.3508 [hep-lat]].
 - [20] C. Bernard *et al.* [MILC Collaboration], *Phys. Rev. D* **71**, 034504 (2005) [arXiv:hep-lat/0405029].
 - [21] M. Cheng *et al.*, *Phys. Rev. D* **74**, 054507 (2006) [arXiv:hep-lat/0608013].
 - [22] A. Bazavov *et al.*, *Phys. Rev. D* **80**, 014504 (2009) [arXiv:0903.4379 [hep-lat]].
 - [23] S. Borsanyi *et al.*, arXiv:1007.2580 [hep-lat].
 - [24] A. Bazavov, T. Bhattacharya, M. Cheng, N.H. Christ, C. DeTar, S. Gottlieb, R. Gupta, U.M. Heller, C. Jung, F. Karsch, E. Laermann, L. Levkova, C. Miao, R.D. Mawhinney, S. Mukherjee, P. Petreczky, D. Renfrew, C. Schmidt, R.A. Soltz, W. Soeldner, R. Sugar, D. Toussaint, W. Unger and P. Vranas.